NO Intercalation Properties of Double-Layered Cuprate, $La_{2-x}Ba_xSrCu_2O_6$. Effect of Treatment with Water Vapor

Masato Machida,* Hirotaka Murakami, Takeshi Kitsubayashi, and Tsuyoshi Kijima

Department of Materials Sciences, Faculty of Engineering, Miyazaki University, 1-1 Gakuen-Kibanadai-Nishi, Miyazaki 889-21, Japan

Received July 12, 1995. Revised Manuscript Received October 23, 1995[⊗]

The NO intercalation properties of substituted double-layered cuprates, $La_{2-x}Ba_xSrCu_2O_6$, have been studied by means of XRD, ED, HREM, and FT-IR. The NO absorbability was strongly influenced not only by the amount of Ba substitution but also by the pretreatment with saturated water vapor at 60 °C. The Ba substitution leads to $\sqrt{2}a \times \sqrt{2}a$ and $3a \times 3a$ superstructures, which are associated with the ordering of Ba and oxygen vacancies, respectively. The sample with the superstructure showed rapid NO uptake at 250 °C only after water vapor treatment. The XRD measurement demonstrates a two-stage lattice expansion along the *c* axis after reactions with water vapor and subsequently with NO. The parallel HREM study suggests that the expanded structure is due to the insertion of H_2O and NO species into interlayers between bottom planes of CuO_5 pyramids. Aging the sample in water vapor leads to the formation of interlayer hydroxyl groups, which are effective in promoting NO intercalation by expanding the interlayer spacing between the CuO_5 sheets.

Introduction

Double-layered cuprates have been studied as a relatively new class of superconductors in recent years.[1−5] The wide variety of possible metallic components and the unique open structure of this system are also expected to produce interesting chemical reactivities. We have previously reported that the substituted layered cuprates, $La_{2-x}Ba_xSrCu_2O_6$, absorb large quantities of dilute nitric monoxide from gas phase.[6] The amount of NO uptake strongly depends on the Ba substitution, exceeding 0.9 mol/mol of cuprate at $x = 1.0$. The NO absorption brought about significant expansion of the interlayer spacing of the cuprate without precipitation of other phases.[7] This is in complete contrast to other Ba-containing cuprates, such as the Ba−Y−Cu−O or Ba−Cu−O systems, which absorb gaseous NO via solid-gas reactions to produce $Ba(NO_2)_2$ and/or $Ba(NO_3)_2$.[8−13] More interestingly, part of the NO molecules incorporated into $La_{2-x}Ba_xSrCu_2O_6$ are eliminated dissociatively as O_2 at 620 °C and N_2 at 920 °C.[6] The apparent conversion of absorbed NO to N_2, which is also dependent on the Ba content, reached a maximum (ca. 50%) at $x = 0.5$. Although such irreversible NO intercalation chemistry is considered to result from strong interactions within an interlayer, the whole mechanism has not been elucidated yet. To gain an understanding of this remarkable reactivity of double layered cuprates, a systematic structural characterization is necessary.

In the present work, we have studied the changes in crystal and chemical structure of the $La_{2-x}Ba_xSrCu_2O_6$ attending a course of NO intercalation. Since the NO uptake is increased by Ba substitution, we employed X-ray and electron diffraction to characterize the structure of substituted cuprates. It has become evident that the NO absorbability is affected by exposing the samples to water vapor. This effect of promoting NO absorption is discussed from a structural viewpoint to elucidate the mechanism of NO intercalation.

Experimental Section

The double-layered cuprates, $La_{2-x}Ba_xSrCu_2O_6$, were prepared from powder mixtures of oxides and carbonates. Calculated amounts of La_2O_3, $BaCO_3$, $SrCO_3$, and CuO were mixed together in an automatic mortar grinder overnight and subsequently calcined in dry air at 1050 °C for 10 h. The heating and cooling rate was constant at 5 °C/min. As-prepared dry samples were treated with saturated water vapor (ca. 20 kPa) at 60 °C for 48 h prior to the reaction with NO, which took place in a volumetric vacuum system. After evacuating the sample, 2.63×10^4 Pa of NO (99.9%) gas was introduced at 250 °C and the amount of NO uptake was determined as a function of time on stream.

The crystal structure of the sample was determined by powder X-ray diffraction (XRD, Rigaku RINT-1400) using 30

[⊗] Abstract published in *Advance ACS Abstracts*, December 1, 1995.

(1) Cava, R. J.; Batlogg, B.; van Dover, R. B.; Krajewski, J. J.; Waszczak, J. V.; Fleming, R. M.; Peck, W. F.; Rupp, L. W.; Marsh, P.; James, A. C. W. P.; Schneemeyer, L. F. *Nature* **1990**, *345*, 602.
(2) Kinoshita, K.; Shibata, H.; Yamada, T. *Physica C* **1990**, *171*, 523.
(3) Kinoshita, K.; Shibata, H.; Yamada, T. *Physica C* **1991**, *176*, 433.
(4) Fuertes, A.; Obradors, X.; Navarro, J. M.; Gomes-Romero, P.; Casa-Pastor, N.; Fontcuberta, J.; Miravitlles, C.; Rodriguez-Cavajal, J.; Martinez, B. *Physica C* **1990**, *170*, 153.
(5) Okai, B. *Jpn. J. Appl. Phys.* **1991**, *30*, L179.
(6) Machida, M.; Murakami, H.; Kitsubayashi, T.; Kijima, T. *J. Mater. Chem.* **1994**, *4*, 1621.
(7) Machida, M.; Murakami, H.; Kijima, T. *J. Chem. Soc., Chem. Commun.* **1995**, 485.
(8) Machida, M.; Yasuoka, K.; Eguchi, K.; Arai, H. *J. Chem. Soc., Chem. Commun.* **1990**, 1165.
(9) Machida, M.; Ogata, S.; Yasuoka, K.; Eguchi, K.; Arai, H. *Proc. Int. Congr. Catal.* **1993**, 2645.
(10) Arai, H.; Machida, M. *Catal. Today* **1994**, *22*, 97.
(11) Tabata, K.; Fukui, H.; Kohiki, S.; Mizuno, N.; Misono, M. *Chem. Lett.* **1988**, 799.
(12) Mizuno, N.; Yamato, M.; Misono, M. *J. Chem. Soc., Chem. Commun.* **1988**, 887.
(13) Arakawa, T.; Adachi, G. *Mater. Res. Bull.* **1989**, *24*, 529.

0897-4756/96/2808-0197$12.00/0

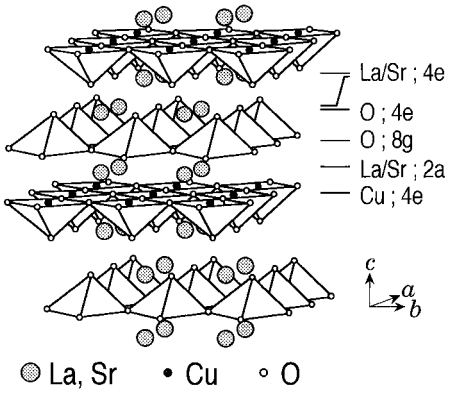

Figure 1. Ideal crystal structure for 2126-type double layered cuprate.

kV × 20 mA Cu Kα radiation. The electron diffraction (ED) study was performed on a JEOL 2000FX electron microscope fitted with a Gatan eucentric goniometer (±30°). High-resolution electron microscopy (HREM) was performed on a JEOL 4000EX electron microscope operated at 400 keV with a top-entry goniometer stage. The sample was crushed and dispersed in dry ethanol and deposited on a holey carbon film supported by a copper grid. All HREM observations were carried out under electron irradiation with a beam current less than 115 μA to prevent damage of the sample.

The chemical structure of the steam-treated and NO-absorbed samples was studied by measuring infrared absorption spectra. A powder mixture of the water-treated sample and KBr pressed into a disc (20 mm) was placed in a temperature-controllable quartz cell with CaF_2 windows, which was connected to an evacuation system. The absorption spectra were recorded on a JASCO FTIR 300 spectrometer after evacuation and/or after introducing NO at elevated temperatures.

Results and Discussion

The crystal structure of the unsubstituted sample, $La_2SrCu_2O_6$, is known as a "2126-type" double-layered structure (I_4/mmm, $a = 0.386$ nm, $c = 1.988$ nm). This structure is regarded as derived from $Sr_2Ti_2O_7$, i.e., formed of double pyramidal copper layers intergrown with rock salt type layers as shown in Figure 1.[14−18] In this structure, large cations, such as La and Sr, are distributed in 4e and 2a sites, whereas Cu occupies the 4e site to form CuO_5 pyramids with oxygens in the apical site (4e) and the corner site (8g). A lanthanum site can be partially replaced by divalent cations as has been reported for $La_{2-x}Sr_xCaCu_2O_6$,[1] $La_{2-x}Ca_{1+x}Cu_2O_6$,[2,3] and $La_{2-x}Sr_{1+x}Cu_2O_6$.[19−21] As is apparent from Figure 1, there are anion-deficient interlayers between the copper planes.

X-ray diffraction patterns for dry samples of $La_{2-x}Ba_xSrCu_2O_6$ are compared in Figure 2a. The Ba substitution retained the double-layered structure but decreased the crystallinity as judged from the broadening of the peaks at higher x values. A weak (002)

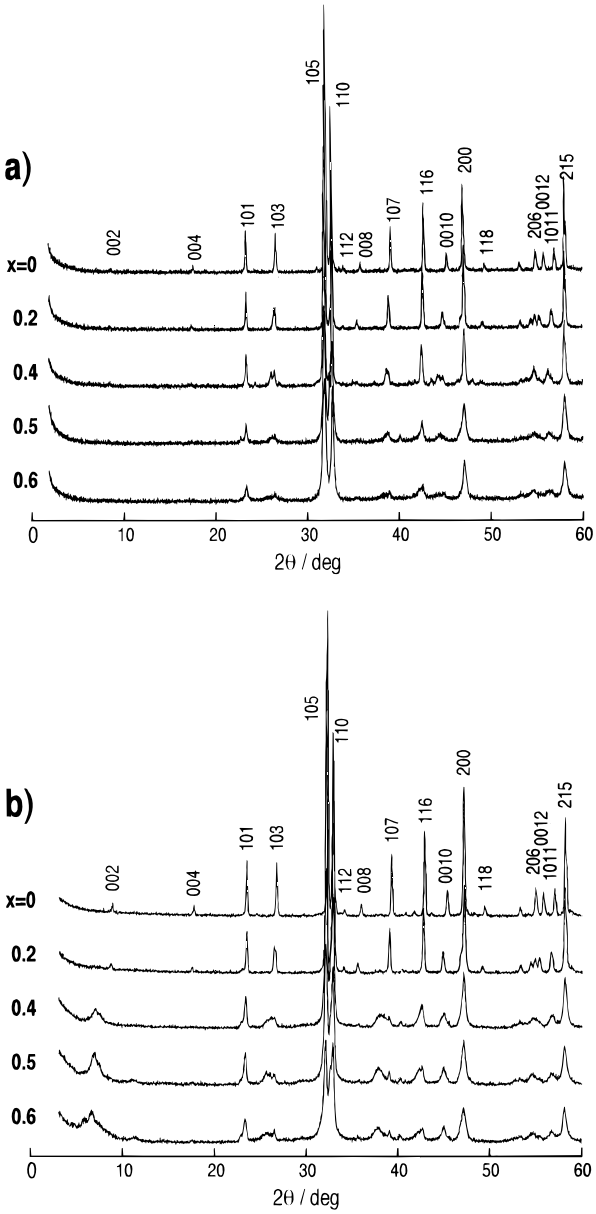

Figure 2. Powder XRD patterns of $La_{2-x}Ba_xSrCu_2O_6$: (a) dried samples; (b) after water vapor treatment (20 kPa, 60 °C, 24 h).

reflection at $2\theta = 8.85°$ is shifted slightly to lower angles by the Ba substitution. This represents the increase in the layer stacking periodicity from 0.994 ($x = 0$) to 1.02 nm ($x = 0.5$), because the ionic radius of Ba^{2+} (0.143 nm) is larger than that of La^{3+} (0.122 nm). A similar XRD pattern was reported for $La_{1.6}Ba_{0.4}SrCu_2O_{6-\delta}$ by Rao et al.,[22] who indicated that the sample was monophasic with a tetragonal (I_4/mmm, $a = 0.384$ nm, $c = 2.020$ nm) structure.

On the other hand, the XRD patterns were apparently modified by the steam treatment (Figure 2b), which caused a shift of the (002) reflection to lower angles at $x \geq 0.4$. The corresponding d value increased from 1.02 to 1.25 nm, suggesting a 23% lattice expansion along the c axis. Actually, a sintered sample, prepared by heating powders pressed into a rectangular shape, was expanded after exposure to water vapor. The effect of steam treatment depends on the Ba content, but the

(14) Nguyen, N.; Er-Rakho, L.; Michel, C.; Choisnet, J.; Raveau, B. *Mater. Res. Bull.* **1980**, *15*, 891.
(15) Doverspike, K.; Liu, J.-H.; Dwight, K.; Wold, A. *J. Solid State Chem.* **1989**, *82*, 30.
(16) Nguyen, N.; Michel, C.; Studer, F.; Raveau, B. *Mater. Chem.* **1982**, *7*, 413.
(17) Michel, C.; Raveau, B. *Rev. Chim. Miner.* **1984**, *21*, 407.
(18) Torrance, J. B.; Tokura, Y.; Nazaal, A.; Parkin, S. S. P. *Phys. Rev. Lett.* **1988**, *60*, 542.
(19) Caignaert, V.; Nguyen, N.; Raveau, B. *Mater. Res. Bull.* **1990**, *25*, 199.
(20) Izumi, F.; Takayama, E.; Nakai, Y.; Asano, H. *Physica C* **1989**, *89*, 157.
(21) Kondo, J.; Asai, Y.; Nagai, S. *J. Phys. Soc. Jpn.* **1988**, *57*, 4334.
(22) Mahesh, R.; Vijayaraghavan, R.; Rao, C. N. R. *Mater. Res. Bull.* **1994**, *29*, 303.

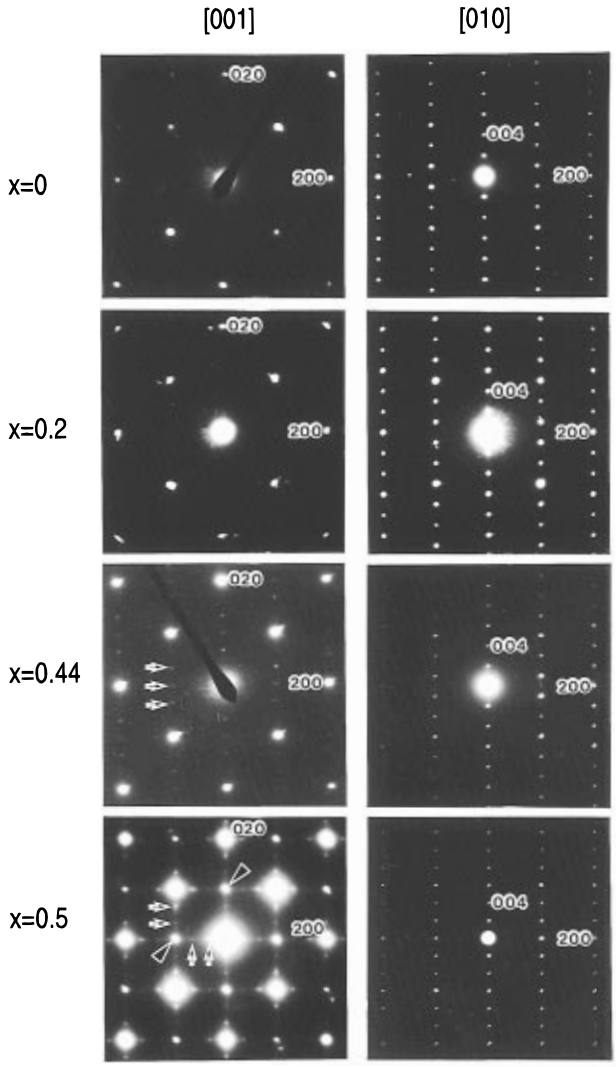

Figure 3. ED patterns of dried $La_{2-x}Ba_xSrCu_2O_6$ samples with incident beams parallel to [001] and [010]. Two types of extra reflection spots are observed for $x = 0.5$; (▲) $\sqrt{2}a \times \sqrt{2}a$, (→) $3a \times 3a$ superlattices.

structural changes due to the substitution is not visible by XRD. Thus, further investigation by ED was carried out to characterize the effect of Ba substitution on the crystal structure.

The ED measurement of more than 50 crystals gave evidence for a single-phase material in agreement with the XRD results. The [001] and [010] ED patterns of dried $La_{2-x}Ba_xSrCu_2O_6$ samples are shown in Figure 3. The conditions of reflection for the unsubstituted sample ($x = 0$) are $h0l$, $h + l = 2n$ and $hk0$, $h + k = 2n$, leading to the I_4/mmm space group, which agrees with the structural analysis by Nguyen et al.[14] Since the same ED pattern is basically retained at $x \leq 0.3$, the crystal structure is essentially the same. On the contrary, the [001] pattern at $x = 0.44$ shows very faint extra reflections indicating 3-fold periodicity along a^* ($a = 3a_{2126}$). These extra spots became more distinct for almost all crystals at $x = 0.5$ and represent two different types of diffraction maxima: (i) Bright spots ascribable to $hk0$, $h + k \neq 2n$, which are forbidden in I_4/mmm. This corresponds to a $\sqrt{2}a \times \sqrt{2}a$ superstructure. (ii) Very weak spots indexed on the basis of $3a \times 3a$ superstructure reflections. This diffraction component is similar to that for $x = 0.44$.

These appeared to be like the "123-type" structure, but the precipitation of second phases such as La-

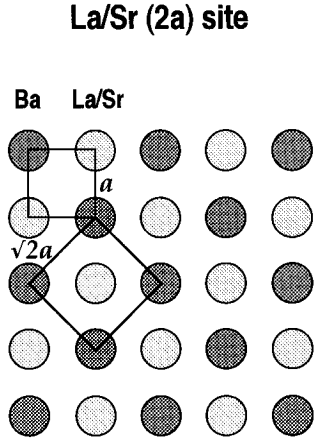

Figure 4. A plausible model of the *ab* planes representing the $\sqrt{2}a \times \sqrt{2}a$ arrangement of Ba in the La/Sr(2a) site.

$(BaSr)_2Cu_3O_7$ was confirmed to be negligible from XRD and EDX analysis. It should be noted that the superstructure spots in Figure 4 violate I-type symmetry and are predominantly primitive in symmetry. The observed reflections for $x = 0.5$ from the [010], [001], [110], and [120] zone axes can be indexed according to a tetragonal cell with the following parameters: $a = 0.545$, $c = 2.040$ nm, with reflection conditions, $hk0$, $h + k = 2n$, $h0l$, hhl, $l = 2n$, and $h00$, $h = 2$, leading to the possible space group P_4/ncc. It should be also pointed out that some I-centered and the intermediate-type ED patterns were observed for a small number of crystals. These results imply that a change of crystal structure from I-centered to the primitive superlattice occurs at $x \approx 0.5$.

Since these extra reflections were retained after the steam treatment, Ba substitution must be responsible for the formation of the superstructure. Taking into account that the strongest $\sqrt{2}a \times \sqrt{2}a$ reflections were obtained for $x \approx 0.5$, the superstructure must be associated with the ordering of cations as observed in several other layered cuprates.[23−25] In the unsubstituted $La_2SrCu_2O_6$, a random distribution of La/Sr between 4e and 2a sites was pointed out by some researchers[14,19,20] and is also supported by the present ED result with the absence of superstructure reflections at $x = 0$. However, substitution of Ba for La may lead to the ordering of Ba in either of these sites, because the ionic radius of Ba^{2+} (0.143 nm) is much larger than Sr^{2+} (0.127 nm) and La^{3+} (0.122 nm). Actually, combining La^{3+} and Ca^{2+} (0.106 nm) in a double-layered structure produces an ordering of La and Ca between the 4e and 2a sites, respectively.[19,20] Supposing a $\sqrt{2} \times \sqrt{2}$-type Ba ordering in the 2a site as one part of the superstructure (Figure 4), the resulting composition is in accord with $x = 0.5$, at which the strongest excess reflections were observed.

Another type of extra reflection, $3a \times 3a$, is considered to be associated with lattice oxygens because of the very weak contrast. It is well-known that the metal oxides tend to produce superstructures based on the ordering of excess oxygen[23] or that of oxygen vacancies.[24] However, since annealing in Ar does not affect the $3a \times 3a$ reflection in the present system, it is attributable to the

(23) Zhou, W. *Chem. Mater.* **1994**, *6*, 441.
(24) Zhou, W.; Dalton, M.; Jefferson, D. A.; Edwards, P. P. *Bull. Mater. Sci.* **1991**, *14*, 567.
(25) Senaris-Rodriguez, M. M.; Alario-Franco, M. A. *J. Solid State Chem.* **1993**, *106*, 134.

ordering of the oxygen vacancies. If lattice oxygens are removed from either 4e or 8g sites to produce the $3a \times 3a$ ordering of O^{2-} vacancies, the resulting stoichiometry should be 5.75. This value agrees with that calculated under the assumption that the valence of the cations are La^{3+}, Ba^{2+}, Sr^{2+}, and Cu^{2+} ($x = 0.5$); however, that obtained from iodometric titration was 6.02. This difference of oxygen content shows the presence of Cu^{3+} and thus excess oxygens. Such oxygen nonstoichiometry is explained by the presence of an intercalated oxygen, which was revealed in a neutron diffraction study of $La_2SrCu_2O_6$ conducted by Caignaert et al.[26] They suggested that the apical oxygen site (4e) of the CuO_5 pyramids is fully occupied, whereas the corner oxygen site (8g) on the copper planes becomes deficient with the simultaneous generation of an interlayer oxygen site between copper planes. Although this will lead to the formation of CuO_5 pyramids sharing their corners along the *c* axis, its contribution to the superstructure of $La_{2-x}Ba_xSrCu_2O_6$ is not understood at the present stage. Here, we must note that we do not claim to have established any further refinements of the crystal structure based on this model. Converting the I to the P lattice cannot be explained by the simple ordering of cations and oxygen vacancies within the layers. It maybe require some displacements of layers sliding along the *ab* plane. Also, the fitting of the XRD patterns to the models proposed above are difficult due to the low crystallinity and the strong affinity of these samples toward water vapor, which causes a drastic deformation of the crystals as discussed below.

It is worth mentioning that, in the $La_{2-x}Ba_xSrCu_2O_6$ system, the high reactivity to water vapor to produce an expanded phase can be observed for the samples with superstructures. Also, the different reactivity to water will affect the NO absorbability. To make this point clear, the effect of steam treatment on the NO uptake was measured in a volumetric vacuum system (Figure 5a), whereas the absorption was scarcely observed for a dried sample ($x = 0.5$) but rose steeply to ca. 0.5 mol/mol over a steam-treated sample. Figure 5b shows the effect of Ba substitution on the NO uptake after the steam treatment. Note that the samples can be classified into two groups from the time course of the NO absorption. The absorption from the first group, with *x* less than 0.4, was extremely slow. The samples in this group are characterized by a normal periodicity of layer stacking (Figure 2b). The second group, $x \geq 0.4$, showed much higher initial absorption rates. Contrary to the first group, these highly substituted samples showed a larger periodicity. Therefore, the expanded lattice, produced at $x \geq 0.4$ after steam treatment, must be responsible for the rapid NO uptake. For every sample, the amount of NO absorption is almost constant after 160 min and nearly equal to the *x* value regardless of the amount of Ba substitution, indicating that an equimolecular reaction between Ba and NO occurs.

The reaction of the substituted cuprates and water vapor proceeds rapidly, so that the sample with a high Ba content, $x = 0.5$ for instance, produced the expanded phase after several days of exposure to moisture in the atmosphere at room temperature. On the contrary, the

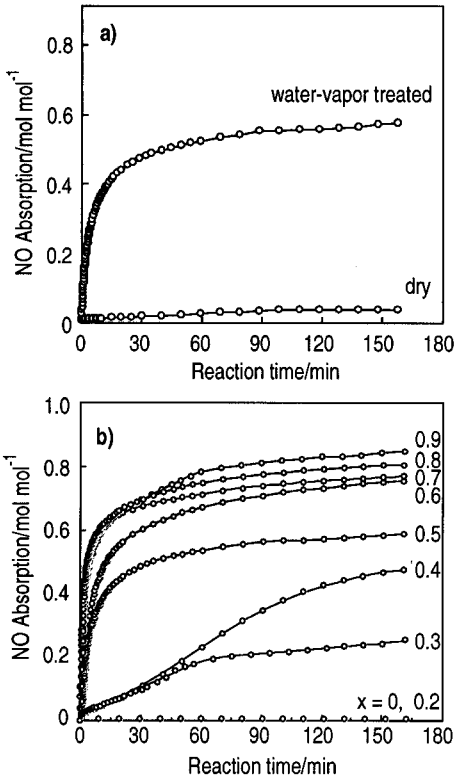

Figure 5. Time courses of NO absorption into $La_{2-x}Ba_xSrCu_2O_6$ measured in a volumetric vacuum system at 250 °C: (a) dried and water-vapor-treated sample ($x = 0.5$), (b) water-vapor-treated sample with various *x*.

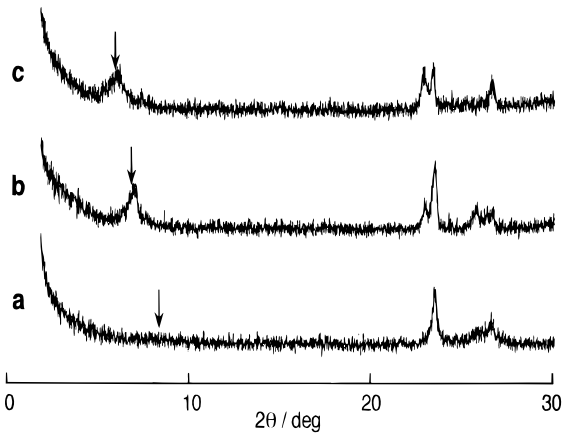

Figure 6. Change of XRD patterns of $La_{1.5}Ba_{0.5}SrCu_2O_6$ during intercalation: (a) a dried sample, (b) a sample on exposure to water vapor (20 kPa, 60 °C, 48 h), and (c) subsequently to NO (13 kPa, 250 °C, 160 min).

expanded phase could not be produced for the sample with low Ba contents ($x \leq 0.3$) even at higher water vapor pressure (10^5 Pa) and/or higher temperatures (100 °C). Abundant Ba species is necessary to demonstrate a sufficient reactivity to water vapor and thus to NO.

The structural change during reactions with water vapor and NO is shown in the XRD patterns in Figure 6. As mentioned above, the diffraction pattern after steam treatment is characterized by the appearance of a new diffraction peak at $2\theta = 7.0°$, corresponding to a long periodicity of 1.25 nm, whereas that of the dried sample is 1.02 nm. A further expansion of the layered structure along the *c* axis was brought about by subsequent reaction with NO at 250 °C. The resultant (002) reflection is situated at 6.3° after absorption of 0.5 mol/mol of NO, corresponding to an interlayer periodicity

(26) Caignaert, V.; Nguyen, N.; Raveau, B. *Mater. Res. Bull.* **1990**, *25*, 199.

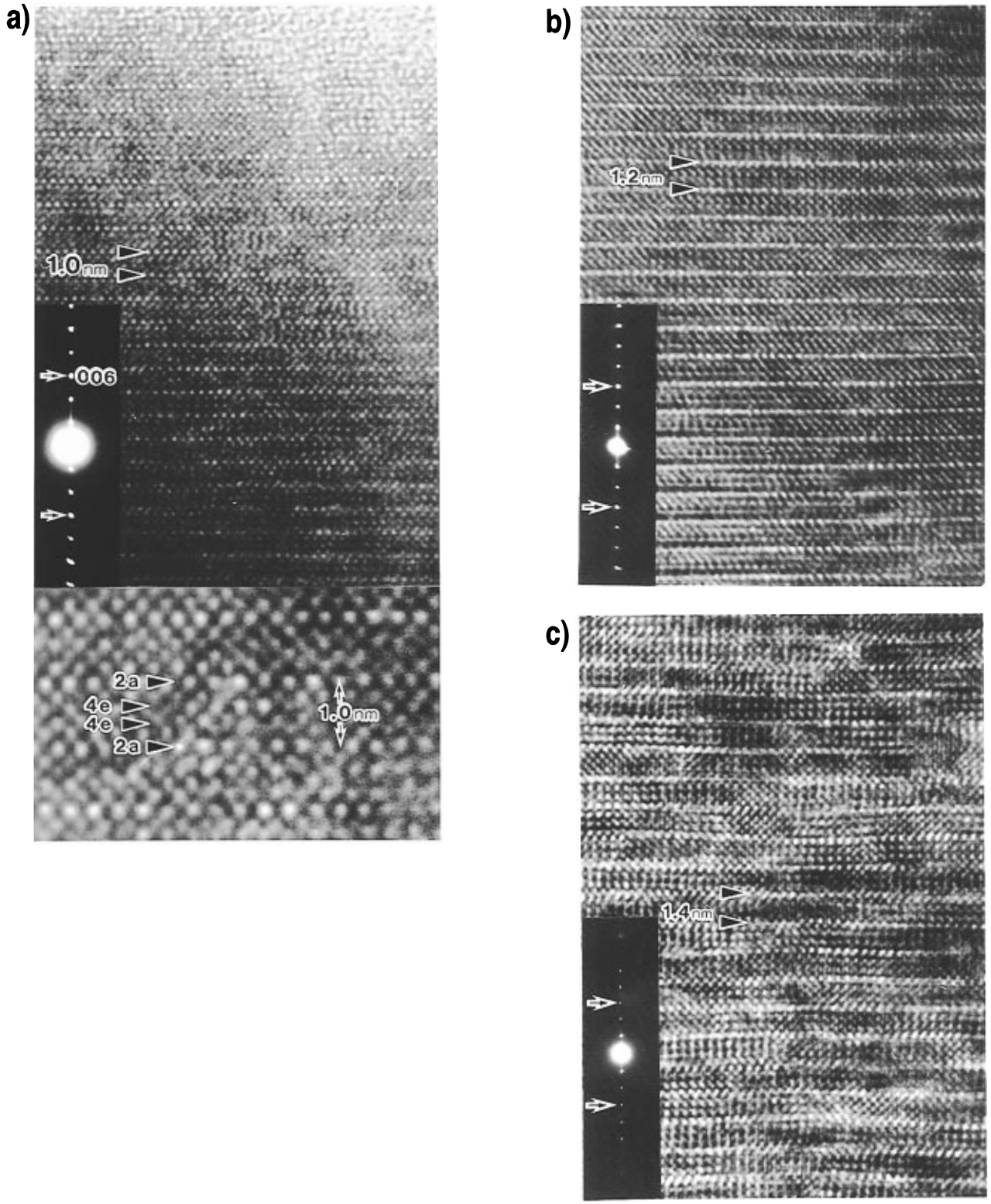

Figure 7. HREM images and [010] ED patterns of (a) $LaSr_2Cu_2O_6$, $La_{1.5}Ba_{0.5}SrCu_2O_6$ (b) on exposure to water vapor (20 kPa, 60 °C, 48 h), and (c) subsequently to NO (13 kPa, 250 °C, 160 min). A lower part of (a) shows that arrays of 2a and 4e sites of La/Sr along [100] constitute an I-centered lattice.

of ca. 1.4 nm. During these processes, the precipitation of second phases was not detectable by XRD.

A parallel HREM observation was performed to obtain a structural image with the incident beam normal to (010) (Figure 7). The structural image of the unsubstituted sample (Figure 7a) was characterized by stacking layers with a periodicity along the *c* axis close to 1.0 nm, showing the contrast of two CuO_5 sheets (dark) between La/Sr(2a) interlayers (bright). The white dots, lined up along the interlayer, are shifted a half periodicity to the *a* direction in one row with regard to the adjacent ones. This is consistent with an ideal double-layer structure with an I-centered lattice (Figure1). In the image of the Ba-substituted ($x = 0.5$) sample after water vapor treatment (Figure 7b), the stacking periodicity expanded to 1.2 nm and white contrast at the interlayer position became intense as compared to that in Figure 6a. In contrast to the $x = 0$ case, the stacking of layers is primitive rather than I-centered as is formed for the dried sample. The

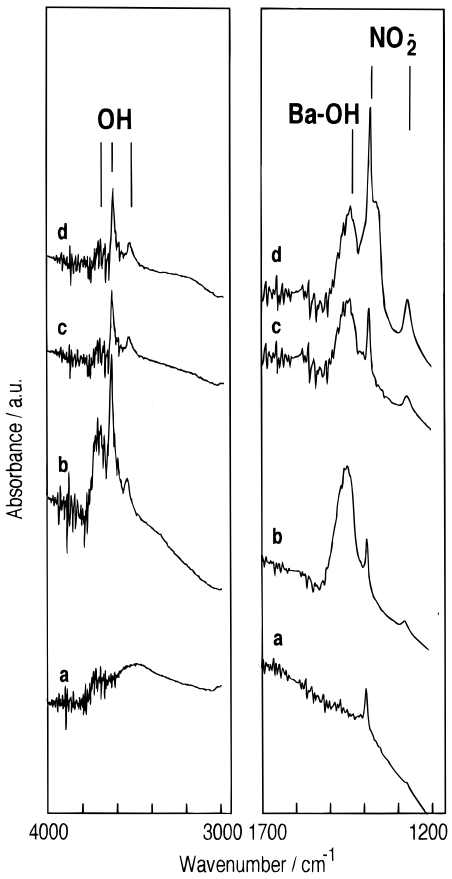

Figure 8. FT-IR spectra of $La_{1.4}Ba_{0.6}SrCu_2O_6$ after water vapor treatment. (a) as treated, (b) after evacuation at 250 °C, (c) after exposing to NO (6.5 kPa, 250 °C, 60 min), (d) after exposing to NO (13 kPa, 250 °C, 60 min).

superstructure ED patterns (Figure 3) were also not influenced by water vapor. Since the image of the structure unit sandwiched between the interlayers is basically unchanged, the lattice expansion can be attributed to an increased thickness of this interlayer region.

After the second lattice expansion through NO absorption (Figure 7c), the structural image became so inhomogeneous and the interlayer periodicity appeared to be fluctuating along the *a* direction. One of the reasons for the deformed structure must be the occurence of precipitous solid−gas reactions in the NO absorption. The initial rate of the NO absorption into the sample ($x = 0.5$) was ca. 1.0 mol/mol of Ba min. The sample was also damaged by electron beam irradiation, which is significant for the NO-absorbed samples. The largest interlayer periodicity observed in the image is about 1.4 nm, which is consistent with the results of XRD observations (Figure 6). The increased bright contrast at the interlayer probably indicates the incorporation of NO molecules between the copper planes. As was speculated from the ED superstructure reflections, this interlayer contains an ordering of Ba ions. Water and NO are considered to be accommodated together into the Ba-containing interlayers between copper planes.

Infrared absorption spectra for $La_{1.4}Ba_{0.6}SrCu_2O_6$ covering the range 1000−4000 cm^{-1} were recorded to analyze the chemical structure of the intercalated species. The sample as treated with water vapor at 60 °C represents a broad OH stretching mode at around 3700−3400 cm^{-1} (Figure 8a). A weak signal at 1380 cm^{-1} is due to nitrate contamination in the KBr. Heating this sample at 250 °C produced new strong peaks at 3680, 3640, and 1445 cm^{-1}. The sharp peaks at ∼3600 cm^{-1} can be also ascribed to OH stretching, but none of these peaks are associated with the KBr matrix. The strong and broad peak at 1445 cm^{-1} became more intense when heated up to 400 °C. A comparison of the spectra for the metal hydroxides of Ba, La, Sr, and Cu revealed that Ba−OH species are responsible for the peak at 1445 cm^{-1}. The characteristic absorption at 1445 cm^{-1} cannot be observed for the sample at $x \leq 0.3$, at which water intercalation negligibly occurred, as is evident from Figure 2b. In addition, XRD and HREM suggest no precipitation of metal hydroxides after the exposure to water vapor. These results suggest that water intercalation and subsequent heating produces Ba−OH species in the interlayer of the bulk materials. The hydroxide group was thermally stable and remained even after evacuating at 700 °C. This is reflected by the extremely high decomposition temperature of barium hydroxide.

After exposing the steam-treated sample to NO at 250 °C, two types of sharp and strong absorptions appeared at 1384 and 1270 cm^{-1}. These absorptions are ascribable to N−O stretching modes of NO_2^- ions.[27] However, since no change was observed for absorptions ascribable to OH species, the direct interaction between the NO and OH in the solid seems unlikely. The formation of nitrite ions is probably a result of interaction between NO and lattice oxygens.

In conclusion, the NO absorption into $La_{2-x}Ba_xSrCu_2O_6$ takes place in two stages of intercalation. In the first stage, water molecules are incorporated between copper planes, producing OH species associated with ordered Ba ions. This structural modification is of particular importance with regard to the NO absorbability, since it induces the expansion of the interlayer, which is effective in accelerating the NO intercalation in the second stage. Barium is indispensable for bringing about both processes because its strongly basic character promotes the reaction with H_2O and NO. Water interaction with cuprate is well-known in high-T_c superconductor corrosion studies.[28,29] A typical "123-type" compound, $Ba_2YCu_3O_{7-\delta}$, for instance, decomposes in water or steam to Y_2BaCuO_5, CuO, $Ba(OH)_2$, and O_2. In this case, it was pointed out that incorporation of OH^- species in oxygen vacancies and/or water intercalation occurs in the initial stage of the reaction. Nitric oxide also shows a strong affinity toward cuprates containing Ba. Machida et al.[89] reported that the simple Ba−Cu−O system, as well as other mixed oxides containing Ba, react easily with gaseous NO to produce $Ba(NO_3)_2$ or $Ba(NO_2)_2$ at 250 °C. Despite the comparable NO absorption rate, the absorption mechanism for $La_{2-x}Ba_xSrCu_2O_6$ is in striking contrast to those materials.

One of the most plausible reasons for the interesting reactivity of this material is double layered structure with a typical two-dimensional character. In this structure, coordinatively unsaturated CuO_5 pyramids

(27) Nakamoto, K. *Infrared and Raman Spectra of Inorganic and Coordination Compounds*, 4th ed.; New York, 1986; p 476.
(28) Yan, M. F.; Barns, R. L.; O'Bryan, H. M.; Gallagher, P. K.; Shewood, R. C.; Jin, S. *Appl. Phys. Lett.* **1987**, *51*, 592.
(29) Qiu, S. L.; Ruckman, M. W.; Brooks, N. B.; Johnson, P. D.; Chen, J. L.; Lin, C. L.; Strongin, M.; Sinkovic, Crow, J. E.; Jee, C. S. *Phys. Rev. B* **1988**, *37*, 3747.

form a sheet, which is independent of the adjacent ones, by sharing corner oxygens. Because of such an open structure, for instance, excess oxygens can enter into the interlayer as reported for $La_{2-x}Sr_{1+x}Cu_2O_6$.[3,15,26] Another point for the characteristic reactivity of the present system is attributable to the superstructure. The $\sqrt{2}a \times \sqrt{2}a$ ordering should play a key role in keeping the adjacent Ba ions isolated. This will be effective not only in attaining an equimolecular reaction between Ba and NO but also in preventing the segregation of Ba species as nitrates or nitrites.

Acknowledgment. Financial support by Nissan Science Foundation is greatly acknowledged. The transmission electron microscope study was carried out in the HVEM Laboratory of Kyushu University.

CM950320V